Control Rod Calibration in TRIGA Reactor Using the Subcritical Multiplication Method

Nuclear Engineering – Politecnico di Milano

Pagliuca Simone, Ronchi Riccardo

simone1.pagliuca@mail.polimi.it, riccardo3.ronchi@mail.polimi.it

Course: Experimental Reactor Kinetics
Academic Year: 2024/2025

ABSTRACT

The accurate calibration of control rods is essential for the safe and efficient operation of nuclear reactors. This study investigates the subcritical multiplication method for control rod calibration in the TRIGA Mark II reactor at LENA, Pavia. A Monte Carlo model was developed using the SERPENT code to estimate control rod worth, and experimental validation was performed. The subcritical multiplication method, which relies on neutron source-driven subcritical multiplication, provides a safe and effective approach for reactivity assessment.

Monte Carlo results exhibited a slight overestimation of control rod worth, which could be mitigated through improved modeling techniques. Despite minor discrepancies, the experimental findings are consistent with alternative calibration methodologies.

Key-words: Control Rod Calibration, Subcritical Multiplication, TRIGA Reactor, Monte Carlo Simulation

NOMENCLATURE

Data & Statistics

$\dot{C}$	Counting rate (cps)
σ_C	Uncertainty in counts
C	Counts per measurement interval
Exp	Experimental data
MC	Monte Carlo simulation

Neutronics Quantities

$\alpha\phi_s$	Calibration factor (s^{-1})
β	Delayed neutron fraction
β_i	Delayed neutron fraction for precursor group i

Λ	Mean neutron generation time (s)
λ_i	Decay constant for delayed neutron precursor group i
ρ	Reactivity
CRW	Control rod worth (dollars)
K	Effective neutron multiplication factor
l	Prompt neutron lifetime (s)
M	Subcritical multiplication factor
n	Neutron population
q	Neutron source strength
T	Reactor period (s)

CONTENTS

1   INTRODUCTION

For the safe operation of a nuclear reactor, it is essential to have precise knowledge of the reactivity characteristics of all control units. The calibration of a control rod enables a quantitative assessment of the reactivity variation induced by the insertion of a neutron absorber into the reactor core.

This study aims to present and validate the subcritical control rod calibration procedure for the TRIGA Mark II Reactor located at LENA, Pavia.

The validation process involves developing a Monte Carlo simulation model using the SERPENT code to estimate the control rod worth. The numerical results are then subjected to experimental validation through dedicated measurements in the reactor facility, ensuring the reliability of the proposed methodology.

1.1   The subcritical method for CR calibration

The subcritical method for control rod calibration relies on the principles of subcritical multiplication, establishing a correlation between reactivity insertion due to control rod movement and a measurable parameter dependent on neutron flux.

By employing an external neutron source, the reactor can sustain a stable neutron flux even while remaining in a subcritical state $(k_{\text{eff}} < 1)$. One of the primary advantages of this method is its safety, as the reactor never reaches a critical or supercritical state during the experiment. Additionally, the procedure is relatively straightforward and requires significantly shorter measurement times compared to alternative calibration techniques.

However, the method has certain limitations, it requires a prior reference calibration, typically obtained using a different approach, and the accuracy of measurements is constrained by the low power levels at which the reactor operates during the experiment.

Furthermore, the precision of the results is influenced by the characteristics of the neutron source and the measurement chain employed.

Despite these challenges, the subcritical method remains a valuable and practical technique for control rod calibration, particularly in TRIGA reactor kinetics studies, where its simplicity and safety provide key advantages.

1.2 TRIGA Reactor Description

The TRIGA (Training, Research, Isotope production, General Atomics) reactor family consists of 66 nuclear research reactors operating in 23 countries, with power ratings ranging from 20 kW to 14 MW. These reactors are primarily used for education and training, materials testing, medical applications, and detector calibration.

The TRIGA Mark II reactor located in Pavia, Italy, reached its first criticality in 1965 and represents one of the latest designs in the TRIGA series. A defining characteristic of TRIGA reactors is their inherent safety, ensuring a self-regulating response to reactivity insertion events. This design principle eliminates the need for complex external safety systems, making them particularly suitable for training environments.

"TRIGA reactors should to be safe even in the hands of young undergraduate students."Frederic de Hoffmann [1]

This philosophy aligns well with their role in academic and research institutions.

The inherent safety of TRIGA reactors is achieved through three fundamental safety functions:

- **Control**: Regulating reactivity.

- **Cooling**: Managing heat removal via natural convection.

- **Containment**: Preventing the release of radioactive materials.

While all three functions are essential for reactor safety, this study focuses primarily on reactivity control, as it is directly relevant to the calibration of control rods.

1.2.1 Control Safety Function in the TRIGA Reactor

In the TRIGA reactor, the control safety function is ensured through three primary components: fuel (prompt effect on reactivity), moderator (thermally induced effects), and control rods.

Fuel and Moderator   Fuel and Moderator are inherently coupled, as they are blended within the fuel elements. Their combined effect on reactivity must ensure a prompt, large, and negative temperature reactivity feedback which limits the temperature excursions during reactivity insertion events, assuring self-regulation.

This characteristic is achieved through the use of uranium-zirconium hydride (UZrH) fuel, where hydrogen serves as a solid moderator, while zirconium stabilizes the chemical structure. The contribution of this fuel composition to the temperature feedback accounts for approximately $50-80$% of the total reactivity coefficient.

The TRIGA fuel elements are cylindrical rods with a height of $70cm$ and a diameter of $3.8cm$, cladded with either aluminum (type 101) or stainless steel (type 103). The UZrH fuel contains 8% uranium by weight, enriched to 19.95%. Graphite is used as both the upper and lower reflector, and burnable poisons or a central zirconium rod may be incorporated.

---

[1]Frederic de Hoffmann (1924–1989) was a nuclear physicist involved in the Manhattan Project and later played a role in founding General Atomics. See: [1].

	101-type	**103-type**
Cladding	Aluminium	304 SS
Zr:H Ratio	1:1	1:1.6
Other Features	2 disks of SmO_3	Zr Central Rod

Table 1: Comparison of 101-type and 103-type fuel elements present in Pavia.

For type 103 fuel elements, the Zr-H ratio is tuned to 1:1.6 to prevent any phase transitions in the crystal structure during transients. These fuel elements, located in the core's inner region, experience the most significant temperature variations.

Control Rods   The TRIGA reactor's reactivity control system consists of three control rods:

- **TRANSient rod** serves as the safety rod and remains outside the core during normal operation.

- **SHIM rod** compensates for large reactivity variations.

- **REGulating rod** is used for fine adjustments, managing small transients and stabilizing reactor power.

The position of the control rods is measured relative to full insertion, which corresponds to complete coverage of the active fuel length. Their position is displayed digitally on the control console in units known as *digits*.

Rod	**Material**	**Composition**	**CRW**
SHIM	B_4C	$15.8\%^{10}B$	$3 \sim 3.5$ \$
REG	B_4C	$15.8\%^{10}B$	$1 \sim 1.5$ \$
TRANSIENT	Borated Graphite	$72\%C + 5.35\%^{10}B + 21.7\%^{11}B$	2 2.5 \$

Table 2: Control Rods and their characteristics

2   THEORETICAL BACKGROUND

The theoretical and experimental framework of this study is based on the subcritical multiplication theory. This theory states that, in a nuclear reactor, a steady neutron flux can be maintained even in a subcritical state $(k_{\text{eff}} < 1)$.

This behavior is possible due to the presence of an external neutron source, which introduces an additional term in the neutron population equation of the Point Kinetics model:

$$\frac{dn}{dt} = \frac{\rho - \beta}{\Lambda}n + \sum_{i=1}^{6} \lambda_i C_i + \mathbf{q} \tag{1}$$

2.1 Neutron Sources

Neutron sources play a crucial role in reactor operation, particularly in start-up procedures and in sustaining and monitoring the neutron flux under subcritical conditions. The design of neutron sources considers two primary parameters:

- **Location** – Proper positioning ensures optimal neutron flux distribution.

- **Intensity** – Sufficient source strength is required to maintain detectable neutron levels.

Neutron sources can be either internal or external to the reactor core.

In the first case, neutrons are generated by materials that are an integral part of the reactor, such as fissile material or through (α, n) and (γ, n) reactions involving activated materials.

On the other hand, an external source can rely on primary sources, such as spontaneous fission from elements like Californium (^{252}Cf), or on a combination of elements such as Radium and Beryllium, which produce neutrons via the (α, n) reaction. Additionally, secondary sources, such as Antimony-Beryllium, undergo the (γ, n) reaction after irradiation, providing an alternative means of neutron generation.

For this study, the neutron source is external and primary, produced through the (α, n) reaction between Radium ^{226}Ra and Beryllium ^{9}Be:

Radium undergoes α decay with a half-life of $T_{\frac{1}{2}} = 1600$ years:

$$^{226}_{88}\text{Ra} \rightarrow ^{222}_{86}\text{Rn} + \alpha \tag{2}$$

The emitted α particles, with an energy of 4.784 MeV (branching ratio: 94.5%), interact with beryllium to produce neutrons via the following reaction:

$$\alpha + ^{9}_{4}\text{Be} \rightarrow ^{12}_{6}\text{C} + n \tag{3}$$

The resulting neutrons can reach a maximum energy of 13 MeV.

Even in a subcritical state, the injected neutrons interact with the fuel, leading to a neutron population stabilization at a level higher than the source alone would provide.

2.2 Subcritical Multiplication Theory

The subcritical multiplication theory can be analyzed within two different domains:

2.2.1 Neutron Generations Domain

When considering neutron generations, the neutron population follows a geometric progression with a ratio k:

$$n = S(1 + k + k^2 + ... + k^n) \tag{4}$$

For a subcritical system $(k < 1)$, the series converges to a finite asymptotic value:

$$n_\infty = \frac{S}{1-k} \tag{5}$$

This allows for the definition of the subcritical multiplication factor M:

$$M = \frac{1}{1-k} \tag{6}$$

A useful parameter to quantify the deviation from criticality is the **subcritical margin**:

$$\text{Subcritical Margin} = 1 - k \tag{7}$$

This margin influences both the subcritical multiplication factor M and the number of generations required to reach the steady-state neutron population. Figure 1 illustrates how neutron population varies over generations for different values of k.
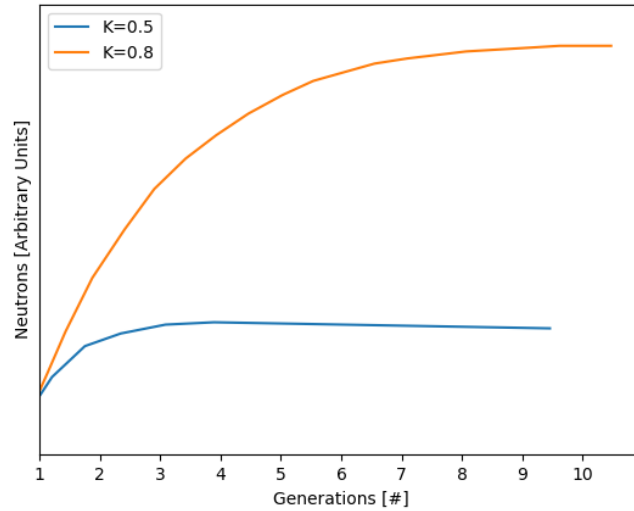

Figure 1: Neutron population over generations for different values of k.

2.2.2 Time Domain

When considering time as the primary domain, the Point Kinetics equations must be solved, incorporating the external neutron source term:

$$\begin{cases} \frac{dn}{dt} = \frac{\rho - \beta}{\Lambda} n + \sum_{i=1}^{6} \lambda_i C_i + q = k \left(\frac{k-1}{k} + \rho - \beta \right) \frac{n}{l} + \sum_{i=1}^{6} \lambda_i C_i + q \\ \frac{dC_i}{dt} = \frac{\beta_i}{\Lambda} n - \lambda_i C_i = k \frac{\beta_i}{l} n - \lambda_i C_i \end{cases} \tag{8}$$

The steady-state neutron population can be derived as:

$$n_\infty = q\frac{l}{1-k} \tag{9}$$

Knowing the definiton of mean generation time and reactivity:

$$\Lambda = \frac{l}{k} \tag{10}$$

$$\rho = \frac{k-1}{k} \tag{11}$$

The steady-state neutron population can be expressed as:

$$n_\infty = -q\frac{\Lambda}{\rho} \tag{12}$$

Using the Laplace Transform, the time-dependent solution for $n(t)$ is obtained:

$$n(t) = q\left(\mathbf{A_0} + A_1 e^{s_1 t} + A_2 e^{s_2 t}\right) \tag{13}$$

The complete formulation is:

$$n(t) = q\left(-\frac{\Lambda}{\rho_0} + \frac{\frac{\beta}{\rho_0}}{\frac{\lambda\rho_0}{\beta-\rho_0}+\frac{\beta-\rho_0}{\Lambda}}e^{\frac{\lambda\rho_0}{\beta-\rho_0}t} + \frac{\frac{\lambda\Lambda}{\beta-\rho_0}-1}{\frac{\lambda\rho_0}{\beta-\rho_0}+\frac{\beta-\rho_0}{\Lambda}}e^{-\frac{\beta-\rho_0}{\Lambda}t}\right) \tag{14}$$

where s_1 and s_2 are the roots of the characteristic equation. The external source does not alter these exponential terms but introduces an integrator, leading to a **constant offset**.

The influence of the subcritical margin is evident in both the steady-state population and the settling time. Figure 2 presents the normalized neutron population over time following a sudden doubling of the neutron source strength for different values of k.
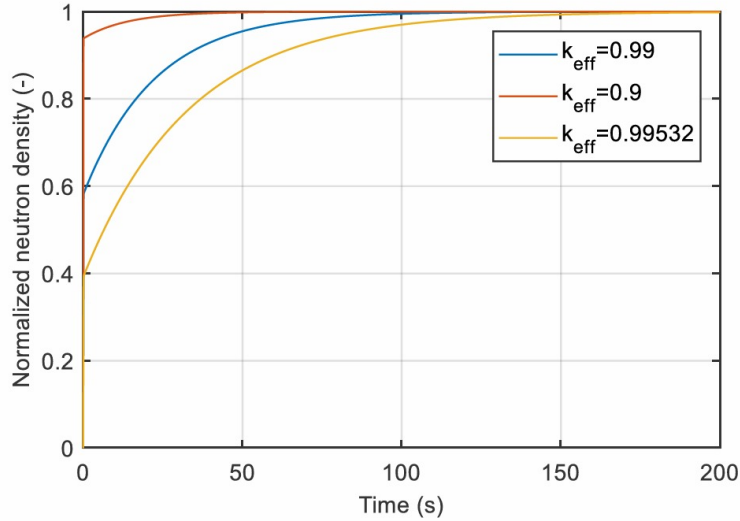
Figure 2: Time evolution of neutron population following a source strength doubling for different values of k.

This highlights two key effects of the multiplication factor:

- As k approaches 1, the **settling time increases**.

- As k increases, the **prompt jump** in neutron population decreases.

2.2.3   Multiple Precursor Groups: In-Hour Equation

This analysis assumes a single group of delayed neutron precursors for mathematical simplicity. However, a more accurate model should consider multiple precursor groups. The proper approach in such cases involves solving the *In-Hour Equation*:

$$\rho = \frac{\Lambda}{T} + \sum_{i=1}^{6} \frac{\beta_i}{1 + \lambda_i T} \tag{15}$$

While the steady-state neutron population remains unchanged, incorporating multiple precursor groups results in a longer settling time compared to the single-group approximation.

3   MONTE CARLO SIMULATION

To complement the experimental results, a Monte Carlo simulation of the TRIGA Mark II reactor was developed using the SERPENT code. The core was modeled with reasonable fidelity to the real geometry, as illustrated in the following plots:
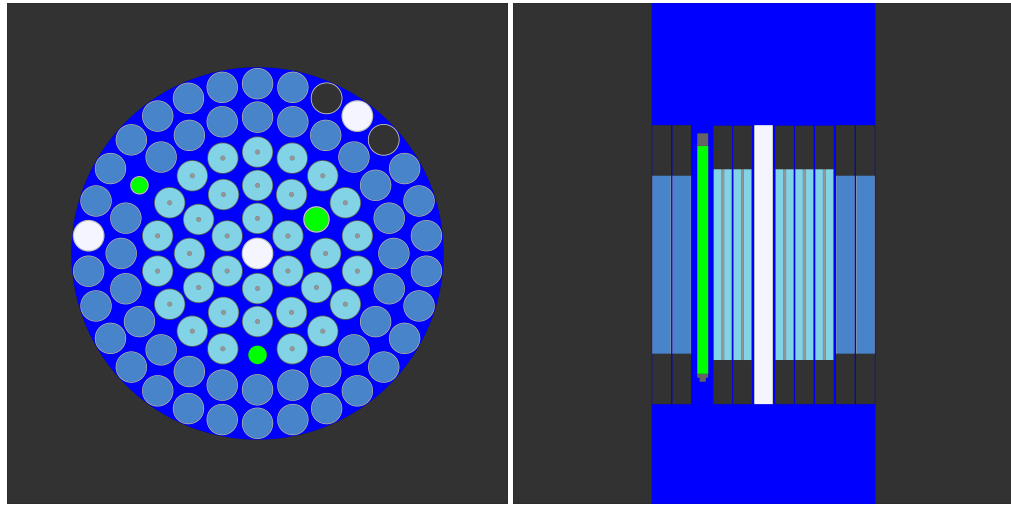

Figure 3: Horizontal and vertical section of the SERPENT geometry

3.1   Simulation Methodology

The Monte Carlo model of the TRIGA core was first benchmarked against criticality calculations to ensure its validity, based on experience gained from the reactor period calibration of the REG

control rod [2].

The simulation was initialized using the following command: `set pop 1000000 5000 20` which sets a population of 1 million neutrons, 5000 cycles, and 20 inactive cycles.

The results were then normalized with: `set power 10` where power is in watts.

The obtained results indicate an overestimation of the control rod worth, where $k_{\text{eff, implicit}}$ from the simulation was taken as the result. The discrepancy in reactivity $\left(\rho = \frac{k-1}{k}\right)$ is shown in Table 3.

Method	Result
Montecarlo	$1.30 \pm 0.03\$$
Experimental	$1.26\$$

Table 3: Control rod worth comparisons between Monte Carlo Criticality simulation and known experimental values, all values are in dollars [\$].

From these values, the overestimation can be quantified as:

$$\frac{\text{CRW}_{MC} - \text{CRW}_{\text{exp}}}{\text{CRW}_{\text{exp}}} = 3.34 \pm 2.55\% \tag{16}$$

which can be attributed to discrepancies between the model and the actual reactor core.

3.2 Subcritical External Source Simulation

After validating the core model, an external neutron source was introduced to simulate the subcritical calibration scenario. The neutron source (4.4 cm in height [3]) was placed in the same channel as in the experimental setup, positioned at the bottom [3]. To enable external source mode, the following parameters were set:

```
src 1 n sm Vacuum_Source
sb 11
...
```

Which defines a neutron source in the specified material (vacuum for simplicity). The energy was defined as a histogram distribution in 11 bins, which was based on literature data [4]. Delayed neutrons were explicitly considered (as they are neglected by default): `set delnu 1`.

The normalization condition was set based on the source emission rate: `set srcrate 1e7`.

The following parameters were set to define the number of neutrons and batches in the external source simulation: `set nps 100000 50`.

To prevent excessive memory usage, constraints were defined for the maximum and minimum time a neutron can be scored [5]:

```
    set tcut 3e-3
    set cfe -1 6E-6
```

All other parameters and geometry remained unchanged.

3.3 Simulated Conditions

The following control rod configurations were simulated:

Configuration	k_{eff}
All in	0.962708 ± 0.00127
Regulating rod out	0.986959 ± 0.00036
Shim rod out	0.974998 ± 0.00069
Transient rod out	0.980734 ± 0.00069

Table 4: Simulated core configurations and resulting k_{eff} values.

From these values, the control rod worth can be calculated as:

$$\rho_i = \frac{k_{\text{eff},i} - 1}{k_{\text{eff},i}} \tag{17}$$

$$\text{CRW}_i = \rho_i - \rho_{\text{all in}} \tag{18}$$

3.4 Comparison with Experimental Data

The results from the Monte Carlo simulations exhibit a systematic overestimation of control rod worth compared to experimental measurements. This discrepancy can be attributed to various factors, including:

- Differences between the modelled and actual core configurations.

- Inaccuracy in neutron source energy spectra.

- Uncertainties in nuclear data libraries.

- Computational limits imposed on the simulation.

	REG			TRANS			SHIM		
	Min	Result	Max	Min	Result	Max	Min	Result	Max
MC	1.58	1.79 ± 0.21	2.00	2.41	2.62 ± 0.21	2.83	3.31	3.50 ± 0.19	3.69
Ref		1.26			2.23			3.22	

Table 5: Control rod worth comparisons between Monte Carlo (MC) simulations and reference experimental values (Ref) provided by LENA, all values are in dollars [$].

3.5 Observations

The Monte Carlo model provides a valuable tool for evaluating control rod calibration procedures. Although the raw simulation results show a slight overestimation, the overall consistency between Monte Carlo results and experimental data supports the validity of the subcritical control rod calibration method used in this study.

Further refinement of the Monte Carlo model could improve accuracy. Particular attention should be given to:

- Refining the simulation time constraints.

- Improving the representation of the reactor's real-state conditions.

- Enhancing the accuracy of neutron source modelling.

4 EXPERIMENTAL CAMPAIGN

The experimental campaign aims to validate the proposed model, which establishes a relationship between reactivity insertion due to control rod movement and a measurable parameter. In this case, the chosen parameter is the counting rate of a fission chamber.

The use of a fission chamber is necessary due to the low reliability of power measurements at extremely low levels and the difficulty in precisely determining the neutron source intensity. By employing this method, variations in neutron flux between different control rod configurations can be inferred.

Since the efficiency of the source-counting system and the exact neutron flux are unknown, this approach is considered an *approximate method*. These uncertainties are managed by computing a calibration factor associated with the fission chamber.

4.1 From Differential to Integral Reactivity Worth

The differential reactivity curve of a control rod can be, in principle, determined by exploiting the relationship between the multiplication factor k and the subcritical multiplication factor M, which links the neutron source intensity to the steady-state neutron population in the core.

By evaluating the reactivity difference between successive extraction steps, the differential reactivity worth can be estimated as:

$$\Delta\rho = \rho_{i+1} - \rho_i \tag{19}$$

However, due to the high uncertainty associated with small step extractions, this experiment was limited to a single extraction step. For each control rod, the reactivity difference was determined by comparing the fully inserted and fully extracted configurations, providing a more robust estimation of its integral worth.

4.2 Calibration Factor Calculation

At steady state, the counting rate is given by:

$$\dot{C}_\infty = \alpha\phi_s M \tag{20}$$

where $\alpha\phi_s$ is the calibration factor, which must be determined through comparison with a known reference condition. The relationship between two different counting rate measurements is expressed as:

$$\gamma = \frac{\dot{C}_{\infty,known}}{\dot{C}_{\infty,ref}} = \frac{M_{known}}{M_{ref}} = \frac{1 - k_{ref}}{1 - k_{known}} \tag{21}$$

The calibration factor is computed by comparing the reference condition (all rods inserted, corresponding to a control rod worth of zero) with a known condition obtained from previous calibration experiments. The steps involved are:

$$\gamma = \frac{\dot{C}_{known}}{\dot{C}_{ref}}$$
$$\downarrow$$
$$\rho_{ref} = -\frac{CRW_{ref} - 1}{2} - \frac{1}{2}\sqrt{(CRW_{ref} - 1)^2 + 4CRW_{ref}\frac{\gamma}{\gamma - 1}}$$
$$\downarrow$$
$$k_{ref} = \frac{1}{1 - \rho_{ref}}$$
$$\downarrow$$
$$M_{ref} = \frac{1}{1 - k_{ref}}$$
$$\downarrow$$
$$\alpha\phi_s = \frac{\dot{C}_{ref}}{M_{ref}} \tag{22}$$

This highlights the necessity of prior calibration for at least one control rod to obtain meaningful results.

4.3 Control Rod Worth Estimation

Once the steady-state counting rate is measured and the calibration factor is determined, the subcritical multiplication factor M, the effective multiplication factor k, and reactivity ρ can be computed as follows:

$$M_i = \frac{\dot{C}_i}{\alpha\phi_s}$$
$$\downarrow$$
$$k_i = 1 - \frac{1}{M_i}$$
$$\downarrow$$
$$\rho_i = \frac{k_i - 1}{k_i}$$
$$\downarrow$$
$$\text{CRW} = \rho_i - \rho_{ref} \quad [\text{pcm}] \tag{23}$$

This methodology ensures a systematic approach for determining the reactivity worth of each control rod based on measured neutron counting rates.

> **Application to SHIM Rod Calibration**: The experimental procedure provides a rapid but approximate determination of the integral control rod worth. Given the subcritical nature of all procedural steps, this method can also be applied to calibrate the SHIM control rod. This is particularly relevant since alternative calibration techniques, such as the reactor period method, may encounter difficulties due to the high reactivity worth of the SHIM rod.

4.4 Instrumentation

The experimental setup consists of the following components:

- Reactor and reactor operator.

- Control rods and control panel.

- Neutron source: Radium–Beryllium, activity $2\ Ci$, neutron emission rate: $10^7\ \frac{n}{s}$, placed in the outermost ring (F).

- Fission chamber and its counting chain, operated in pulse mode. A timer is incorporated for setting the measurement time.

- Previous calibration data of the control rods.

4.5 Procedure

1. **Bring the reactor to a cold subcritical condition with all control rods inserted.** Ensure that the fuel temperature is close to room temperature to confirm a "cold" condition. Verify that the reactor is in a "clean" state by checking radioactivity and conductivity measurements of the cooling water.

2. **Measure the natural background counting rate.** This measurement is performed before inserting any neutron source.

3. **Insert the Ra-Be source into the F ring and measure the counting rate.** This configuration serves as the reference measurement.

4. **Calculate the calibration factor by comparison with a known configuration.** The previous calibration of any control rod can be used. For example, if the REG calibration is employed, the measurement should be taken with the REG rod fully extracted while keeping all other control rods inserted.

5. **Perform a control rod extraction step.** Any control rod can be calibrated using this approach. For this specific experiment, only a single extraction step is performed, where the control rod is fully removed.

6. **Wait for the steady-state condition and measure the counting rate.** Steady-state achievement is confirmed by monitoring power behavior. A fixed measurement time of 100 seconds is used, with multiple measurements taken to improve statistical accuracy.

7. **Compute the relevant parameters from the recorded data.** M, k, and finally ρ.

8. **Repeat Step 6 for successive extraction steps.** Not required in this specific experiment, as only a single extraction step is considered.

4.6 Results Collection

Following the described procedure, experimental data were recorded for all possible control rod configurations.

	All in	Reg out	Trans out	Shim out
Integral Counts	60	76	167	261
	71	69	123	303
	92	102	156	211
	59	90	122	219
	59	87	214	228
	77	111	119	243
	52	67	160	332
	65	89	164	239
	45	96	159	244
	68	93	108	241
	37	80		
	52	80		
	72	85		
	64	85		
	67	91		
	68	86		
	66	101		
	66	113		
	64	80		
	54	90		
$\langle C \rangle \pm \sigma_{\langle C \rangle}$	62.9 ± 1.8	88.6 ± 2.1	149.2 ± 3.9	252.1 ± 5.0
$\dot{C} \pm \sigma_{\dot{C}}$	0.63 ± 0.02	0.89 ± 0.02	1.49 ± 0.04	2.52 ± 0.05

Table 6: Counts, average counts, standard deviation, and counting rate for different control rod configurations. Data for TRANS and SHIM rod were taken by half of the groups during the data collection

The raw data consists of N integral neutron counts C, each measurement performed over a 100-second interval (Δt). The count rate $\dot{C}$ and its error were computed using the following formulas:

$$\langle C \rangle = \frac{\sum C}{N} \tag{24}$$

$$\sigma_{\langle C \rangle} = \sqrt{\frac{\langle C \rangle}{N}} \tag{25}$$

$$\dot{C} = \frac{\langle C \rangle}{\Delta t} \tag{26}$$

$$\sigma_{\dot{C}} = \frac{\sigma_{\langle C \rangle}}{\Delta t} \tag{27}$$

5 DATA ANALYSIS

Based on the collected data and the outlined procedure, the control rod worth (CRW) is esti-mated for each control rod. The results are then converted into dollars by normalizing with the known value of the delayed neutron fraction β:

$$\text{CRW [\$]} = \frac{\text{CRW [pcm]}}{\beta} \qquad (28)$$

The values computed by using the REG as a reference are reported in the following table:

	Reg	Trans	Shim
$\alpha\phi_s$		0.019 ± 0.003	
M	46.71 ± 6.06	78.71 ± 10.25	132.99 ± 17.18
K	0.98 ± 0.0028	0.99 ± 0.0017	0.99 ± 0.00097
ρ	-0.022 ± 0.0029	-0.013 ± 0.0017	-0.0076 ± 0.00099
CRW	1.26 ± 0.70	2.49 ± 0.62	3.22 ± 0.59

Table 7: Table of calculated values for different control rods, using experimental calibration results.

5.1 Calibration with different reference values

The same procedure can be applied using the previously obtained calibration of the SHIM and TRANS rods, leading to the following results:

Reference Calibration	Calibration Factor $\alpha\phi_s$	Control Rod	CRW [$]
REG Rod	0.018957 ± 0.002415	REG	3.22±0.59
		TRANS	2.49±0.62
		SHIM	3.22±0.59
TRANS Rod	0.018963 ± 0.001155	REG	1.13±0.39
		TRANS	2.23±0.35
		SHIM	2.88±0.33
SHIM Rod	0.017027 ± 0.001325	REG	1.26±0.36
		TRANS	2.50±0.31
		SHIM	3.22±0.30

Table 8: Calibration factors and control rod worth (CRW) values for different reference cali-brations.

This analysis allows the estimation of control rod worth using different reference calibrations, ensuring consistency and reliability in the evaluation of reactivity control.

5.2 Considerations

The control rod selected as the reference for calibration inherently produces exact results for its own computed worth. However, when using one control rod as a reference to calibrate others, the accuracy of the results is influenced by statistical uncertainties.

It is important to note that the similarity between the values obtained using the REG rod as a reference and those obtained using the SHIM rod is purely coincidental. This is evident from the significantly larger associated uncertainties in the first case.

A consistent trend observed in the results is that the control rod with the lowest reactivity worth exhibits the highest relative error. This occurs because the difference in neutron population between the fully inserted and fully extracted configurations is smaller, leading to lower counting rates. Consequently, the measurement becomes more susceptible to statistical fluctuations.

For the same reason, the lowest uncertainties were found when the SHIM rod was used as a calibration reference, while the highest uncertainties were observed when the REG rod was used.

Finally, a notable observation is the generally high relative errors in the computed values. This outcome is expected, as the recorded counting rates are relatively low. Due to Poisson statistics, the relative uncertainty increases as the magnitude of the measurement decreases. Potential improvements to mitigate this issue include increasing the measurement duration, using a more sensitive detector, or optimizing detector placement.

5.3 Effect of Reactor Clean state on Measurements

If the reactor is not in a clean condition, it implies the accumulation of neutron poisons due to the buildup of fission products. This accumulation leads to a reduction in the number of available neutrons, accordingly decreasing detection efficiency.

Since the distribution of neutron poisons follows the neutron flux, certain regions of the core will exhibit higher concentrations of poisons. This variation affects the flux distribution, consequently altering control rod effectiveness. For instance, the SHIM rod, which has the highest control rod worth (CRW) due to its location in a high-flux region, will experience greater poison production. As a result, its effectiveness might be noticeably impacted.

A quantitative estimation of this effect could be obtained by analyzing the reduction in the SHIM rod's CRW (provided it is not used as a reference). Any observed decrease in its worth could be attributed to negative reactivity insertion due to poison buildup. However, for such an analysis to be reliable, it is essential to first validate the method under clean reactor conditions to establish a baseline reference.

5.4 Sources of Error and Uncertainties

Before discussing the details of error propagation, it is important to acknowledge that since the counting rate was obtained using a fission chamber, the calibration values determined in this experiment are only valid for the present conditions. For any future experiments, the calibration factor must be recomputed to account for potential degradation due to the burnup of fissile material in the fission chamber. However, during the short duration of the measurements, the burnup is assumed to be negligible.

Neglected Uncertainties   Several uncertainties were not explicitly accounted for in our analysis, including:

- Uncertainty in β from Monte Carlo simulations.

- Errors in the measurement chain beyond intrinsic Poisson uncertainty (e.g., timing errors).

- Uncertainty in the known CRW values.

- Shadowing effects, which were not considered.

5.4.1 Statistical Treatment and Error Propagation

The raw data analysis was performed using Poisson statistics, where the standard deviation of the counts is given by:

$$\sigma_{\dot{C}} = \sqrt{\dot{C}} \tag{29}$$

To propagate errors through subsequent calculations, the root sum square (RSS) method was employed:

$$\sigma_f = \sqrt{\sum_i \left(\frac{\partial f}{\partial x_i} \sigma_{x_i} \right)^2} \tag{30}$$

where σ_f is the propagated uncertainty of a function f, and σ_{x_i} represents the uncertainty of each variable x_i.

5.4.2 Numerical Implementation

This error propagation methodology was implemented in Python, where the partial derivatives were computed numerically based on [6]. The implementation in Python can be found in the appendix A

6 CONCLUSIONS

This study provided valuable insights into control rod calibration in the TRIGA Mark II reactor, demonstrating the effectiveness of the subcritical multiplication method while maintaining safe conditions.

Monte Carlo simulations showed a systematic overestimation of control rod worth, likely due to modeling approximations, though experimental results remained consistent with theoretical expectations. The choice of reference rod significantly influenced uncertainties, with the Shim rod yielding more precise measurements.

Future improvements should focus on refining Monte Carlo modeling approaches and enhancing experimental procedure to further reduce uncertainties.

ACKNOWLEDGMENTS

A PYTHON IMPLEMENTATION FOR ERROR PROPAGATION

```python
class Measurement:
    def __init__(self, value, uncertainty):
        if uncertainty < 0:
            raise ValueError("Uncertainty must be non-negative")
        self.value = value
        self.uncertainty = uncertainty
        # String representation
    def __str__(self):
        return f"{self.value:.6g} ± {self.uncertainty:.6g}"

    def rss(func, *measurements):
    # Extract nominal values for function evaluation
    nominal_values = [m.value for m in measurements]
    value = func(*nominal_values)

    # Numerical differentiation and uncertainty propagation
    epsilon = 1e-8  # Small step for finite differences
    squared_uncertainty = 0

    for i, m in enumerate(measurements):
        perturbed_values_plus = nominal_values[:]
        perturbed_values_minus = nominal_values[:]
        perturbed_values_plus[i] += epsilon
        perturbed_values_minus[i] -= epsilon

        # Partial derivative approximation
        df_dxi = (func(*perturbed_values_plus) - func(*perturbed_values_minus)) / (2 *
            epsilon)

        # Add contribution to total uncertainty
        squared_uncertainty += (df_dxi * m.uncertainty) ** 2

    total_uncertainty = math.sqrt(squared_uncertainty)

    # Return the resulting measurement
    return Measurement(value, total_uncertainty)

    # Example usage
    k_val = Measurement(1.24, 0.02)
    rho = rss(lambda k: (k-1)/k, k_val)
    print(rho)
    # Output: 0.193548 ± 0.0130073
```

REFERENCES

[1] Unknown, "Frederic de hoffmann obituary," *Sarasota Herald-Tribune*, Oct. 1989, Accessed 31-Jan-2025. [Online]. Available: `https : / / news . google . com . au / newspapers ? id = gbYcAAAAIBAJ&sjid=VHoEAAAAIBAJ&pg=6267,1698262&dq=frederic-de-hoffmann&hl=en`.

[2] S. Lorenzi, *Experimental nuclear reactor kinetics course*, Course held at Politecnico di Milano from September to December 2024, 2024.

[3] R. Ponciroli, "Modellistica orientata agli oggetti del reattore triga mark ii dell'università di pavia," Relatori: Antonio Cammi, Andrea Borio di Tigliole, Andrea Bigoni, Andrea Fusar Poli, Laurea Specialistica Thesis, Politecnico di Milano, 2010. [Online]. Available: `https://www.politesi.polimi.it/bitstream/10589/11402/3/2010_12_Ponciroli.pdf`.

[4] K. Geiger, R. Hum, and C. Jarvis, "Neutron spectrum of a ra-be(⍺, n) source," *Canadian Journal of Physics*, vol. 42, pp. 1097–1100, Feb. 1964, Republished in 2011 by Canadian Journal of Physics. DOI: `10.1139/p64-103`.

[5] Serpent Development Team. "M&c 2013 example inputs." Accessed on 31-Jan-2025, Accessed: Jan. 31, 2025. [Online]. Available: `https://serpent.vtt.fi/mediawiki/index.php/M%26C_2013_example_inputs`.

[6] R. J. Moffat, "Describing the uncertainties in experimental results," *Experimental Thermal and Fluid Science*, vol. 1, pp. 3–17, 1988, Professor of Mechanical Engineering, Stanford University. DOI: `10.1016/0894-1777(88)90043-X`. [Online]. Available: `https://www.sciencedirect.com/science/article/abs/pii/089417778890043X`.

[7] Serpent Development Team. "Serpent monte carlo wiki." Accessed on 31-Jan-2025, Accessed: Jan. 31, 2025. [Online]. Available: `http://serpent.vtt.fi/mediawiki/index.php?title=Main_Page`.

[8] Serpent Development Team. "Serpent monte carlo forum." Accessed on 31-Jan-2025, Accessed: Jan. 31, 2025. [Online]. Available: `https://serpent.vtt.fi/forum/`.

[9] S. Pagliuca. "Magistrale - experimental reactor kinetics code and data." Accessed on 31-Jan-2025, Accessed: Jan. 31, 2025. [Online]. Available: `https://github.com/simo-pagliu/Magistrale/tree/main/Experimental%20Reactor%20Kinetics`.